Cometesimals in the inner Solar System

T. M. Donahue*, T. I. Gombosi* & B. R. Sandel†

* Space Physics Research Laboratory, Department of Atmospheric and Oceanic Science, The University of Michigan, Ann Arbor, Michigan 48109, USA
† Lunar and Planetary Laboratory, The University of Arizona, Tucson, Arizona 85721, USA

A large flux of small comets in the inner Solar System[1] might produce a recognizable Lyman-α signature near 1 AU (ref. 2). We have now examined spectra obtained by the ultraviolet spectrometer (UVS)[3] on the Voyager 2 spacecraft between 1 and 2.5 AU and have found evidence for a very large number of 'cometesimals' with radii between a few metres and a few tens of metres in the neighbourhood of the Earth. The evidence consists of a component in the interplanetary Lyman-α radiation that decreases rapidly (between r^{-3} and r^{-4}) with heliocentric distance. The Lyman-α emission rate in a direction normal to the Sun-spacecraft line and downwind (the anti-apex direction) in the interstellar wind at 1 AU is 640 rayleighs, of which our analysis attributes 477 R to the interstellar medium (ISM) and 163 R to another source. Despite this result we propose that this source consists of comets of a different sort than those proposed by Frank *et al.*[1] and with a flux seven orders of magnitude smaller. We propose that these cometesimals are ice-coated, porous, low density refractory boulders that may be the building blocks of ordinary comet nuclei[4]. We show that the cometesimals required to produce the observed Lyman-α emission can also account for all the lunar craters with diameters between 200 m and 1,500 m produced during the past 3,200 million years at sites such as Mare Tranquillitatis.

In searching the UVS data obtained from Voyager 1 and 2 near 1 AU for a Lyman-α signature near 1 AU we found one sequence of 17 observations made between 1 AU to ~2.5 AU in which the field of view was always in about the same part of the sky, downwind in the ISM. The observations in that sequence that were obtained near 1 AU were made in a direction that was also perpendicular to the Sun-spacecraft line, but away from the geocorona and geotail. All were obtained at distances greater than 10^7 km from Earth, far outside the geocorona. We have corrected the Lyman-α emission rates for variations in solar Lyman-α (ref. 5) and normalized them to a solar flux of 5.43×10^{11} photons $cm^{-2}\ s^{-1}\ Å^{-1}$, which was the representative value for late 1977 when the data were obtained. We have attempted to correct for the phase shift between the solar Lyman-α arriving at Earth and at the spacecraft. We estimate that the uncertainty in this correction is reflected in an uncertainty of ±2.5% in the data plotted in Fig. 1. We also plot five data points, those with vertical arrows, that were obtained in the same general part of the sky, but should contain somewhat more ISM contribution than the rest.

Figure 1 shows the Lyman-α variation expected for the ISM, normalized to 430 R at 3 AU, from a model of Thomas[6]. If, in addition to the ISM, there is a component in the atomic hydrogen local emission rate that varies as $r^{-\gamma}$, then an observation normal to the Sun-spacecraft axis at a distance r from the Sun will yield a column emission rate given by $r^{-(\gamma-1)}$. We also present curves showing the sum of the ISM and this second component of Lyman-α for values of γ between 3 and 5. The curves are normalized to an emission rate of 163 R in excess of the Lyman-α radiation from the downwind ISM at 1 AU. The uncertainty in corrected counting rate of $\pm 0.07\ s^{-1}$, or ±13 R is small enough that the small excess in Lyman-α between 2.3 and 2.7×108 km is probably significant.

We have calculated the rate at which water molecules are produced from clean ice as a function of heliocentric distance. The production rate varies as $r^{-2.3}$ and has a value of 1.17×10^{-5} g $cm^{-2}\ s^{-1}$ (3.90×10^{17} $cm^{-2}\ s^{-1}$) at 1 AU. The curve for $\gamma = 4.3$ in Lyman-α emission rate corresponds to a variation in hydrogen density of $r^{-2.3}$. This will also be the radial dependence of the product of the water production rate and the hydrogen lifetime. The water production rate from the family of cometesimals at heliocentric distance r is given by

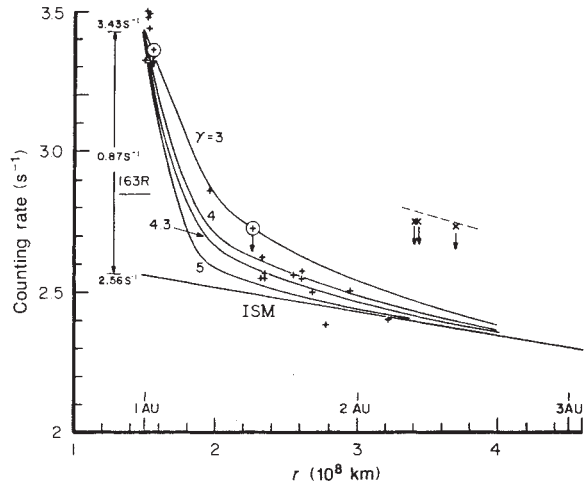

Fig. 1 Lyman-α apparent emission rate observed by the Voyager 2 UVS instrument, days 244–360, 1977. Curves are for ISM Lyman-α alone and ISM plus a contribution varying as $r^{-(\gamma-1)}$. Points with vertical arrows identify observations for which there is a higher ISM contribution by about 10% (dashed line segment).

$$Q(r) = 4\pi a^2 FN = n/(2\tau) \quad (1)$$

where a is the cometesimal radius, N the spatial density of cometesimals, F the water production rate per unit surface area for one cometesimal, n is the hydrogen density and τ the lifetime of hydrogen against ionization (2×10^6 s at 1 AU). Hence, the contribution to the emission rate at 1 AU, from cometesimals of radius a, is given by

$$4\pi I(a) = 8\pi r_o j \tau F f(\gamma) N(a) a^2 \quad (2)$$

per metre of cometesimal radius, where j is the specific Lyman-α emission rate per atom of $2.58 \times 10^{-3}\ s^{-1}$, and r_0 is 1.5×10^{13} cm. For $\gamma = 4.3$ the value of $f(\gamma)$ is 0.72. The differential spatial density $N(a)$ is given by

$$N(a) = \Psi(a)/(2v_r) \quad (3)$$

where $\Psi(a)$ is the sum of inbound and outbound (inactive) cometesimal fluxes per metre of cometesimal radius. In this analysis we have assumed that N is constant and neglect the smearing produced by the motion of the hydrogen atoms. The emission rate is thus proportional to $a^2\Psi(a)$.

There have been numerous observations of the interplanetary Lyman-α radiation between Earth and Venus. We know that the emission rate does not continue to rise as $r^{-(\gamma-1)}$ with $\gamma > 3.5$ inside 1 AU. We are led to conclude that, if cometesimals are the source of the interplanetary hydrogen, a significant fraction of them are losing their clean ice mantles around 1 AU and becoming inactive. Such objects might be porous hydrous silicate boulders with an outer shell of clean ice, whose radii range from tens of centimetres to ~100 m, such as those Gombosi and Houpis[4] have argued may be the building blocks of larger comet nuclei. In this scenario these small cometesimals would be making their first swing through the inner solar system and therefore travelling with near parabolic velocity ($v_r = 30\ km\ s^{-1}$ at 1 AU).

We have attempted to determine a cometesimal flux that is at the same time consistent with lunar cratering rates and the observed Lyman-α production rate. A necessary condition is

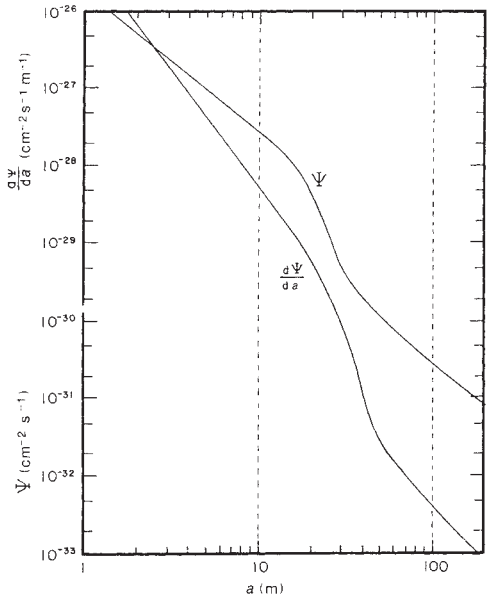

Fig. 2 Differential and integral cometesimal fluxes required to produce lunar crater densities at the Apollo 12 site 3.2×10^9 years old.

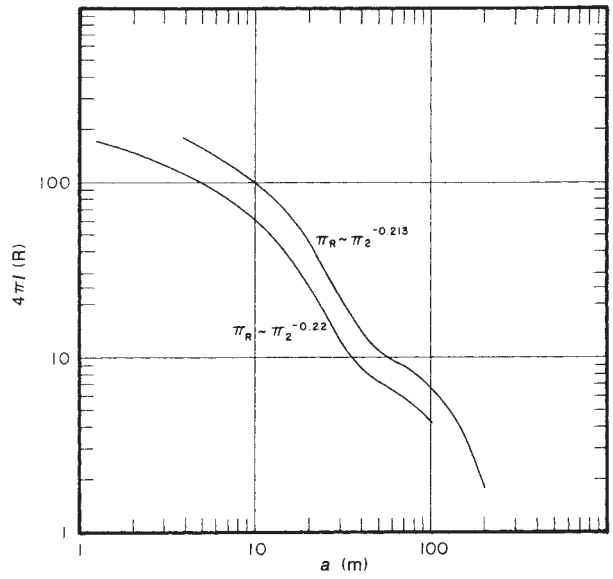

Fig. 3 Integral Lyman-α emission rate from cometesimals with radii greater than a for two assumptions regarding the scaling law for cratering.

that the flux of cometesimals required to produce Lyman-α not produce a higher lunar crater density than the observed one. For the cumulative crater density we have used the lunar calibration curve and chronology presented by Neukum and Wise[7]. We use the cumulative crater density $C(D)$ for craters with diameters greater than D at the Apollo 12 site, 3.2×10^9 years old, to obtain a cratering rate. To relate impactor radius, velocity and density to crater diameter we use the recent experimental scaling laws obtained by Schmidt and Housen[8],

$$\frac{D}{2}\left(\frac{\rho}{m}\right)^{1/3}=0.8\left(\frac{3.22\,g\,a}{u^2}\right)^{-0.22} \quad (4)$$

where ρ is the density of the lunar surface, m the mass of the impactor, u the impact velocity, and g the lunar gravitational acceleration. For u we have averaged impact directions to obtain $u=65$ km s^{-1}. The choice of comet density is crucial. Supported by analysis of comet Halley[9] that cometary densities lie between 0.1 cm and 0.4 g cm^{-3}, we have chosen to use very small values for δ.

The cumulative flux for cometesimals with radii greater than required to reproduce the cratering data is

$$\Psi(a)=4\times10^{-17}\,C(a)\,[\mathrm{cm^{-2}\,s^{-1}}] \quad (5)$$

and the differential flux is

$$\Psi(a)=\frac{d\Psi}{da}=4\times10^{-17}\frac{dC}{dD}\frac{dD}{da}\,[\mathrm{cm^{-2}\,s^{-1}\,m^{-1}}] \quad (6)$$

These limiting differential and integral fluxes are shown in Fig. 2, for $\delta=0.1$ g cm^{-3}. When the corresponding differential Lyman-α production rate from equation (6) is integrated down to $a=3.2$ m (200-m diameter crater), the integral Lyman-α rate is 122 R, of which 114 R is produced by cometesimals with radii less than 40 m (Fig. 3). The crater density curves and corresponding cometesimal flux curves suggest that craters with diameters greater than 1,500 m are created by a different family of impactors than those with diameters less than 1,500 m. According to equation (4) a 1,500-m crater would be created by a cometesimal of 42-m radius. We propose to identify the generators of craters with $D<1500$ m with our cometesimals and suggest that the flux of cometesimals cuts off when the cometesimal radius is large enough to make such a crater. To produce another 50 R of Lyman-α cometesimals with radii as small as 1.25 m would be needed. On the other hand, a change of the exponent in the scaling law to 0.213 would permit cometesimals in the range from 4 m to 50 m to produce 163 R of Lyman-α. Hence, the intriguing conclusion is reached that the same family of cometesimals that accounts for the observed excess of interplanetary Lyman-α radiation above the ISM contribution at 1 AU will also produce all of the craters with radii less than 1,500 m that have appeared on the Moon during the past 3.2×10^9 years. Craters whose diameters are smaller than 200 m could be produced by cometesimals that have become inactive before reaching 1 AU.

We have also calculated the total amount of ice that would be lost by these cometesimals by the time they reach 1 AU. Cometesimals with perihelia between 1 AU and 0.5 AU would lose between 1.6 m and 2.3 m of ice between the Oort cloud and 1 AU. Hence, a low radius cutoff of a few metres for active comets at 1 AU is not unreasonable. Because of the strong dependence of Lyman-α production rate on cometesimal radius in this model, depending as it does on a $a^2\Psi$, the failure of the Lyman-α emission rate to continue to vary as a high power of r inside 1 AU can be accounted for fairly naturally. The average distance between the smallest active cometesimals at 1 AU is only $\sim10^{-2}$ AU and it increases to $\sim10^{-1}$ AU for the largest. Thus, the implicit assumption in our treatment that the hydrogen distrbution is homogeneous is easily satisfied. The interval between impacts on Earth for all cometesimals is about 80 years and for those with radii greater than 30 m is about 10^4 years.

We prefer the model presented here for the source of the extra component of interplanetary Lyman-α to the small comets of Frank *et al.*[1] for the reasons given by Donahue[2]. To hold Lyman-α down to 163 R from the small comets of Frank *et al.*[1] the water production rate would need to be less than 10^{10} cm^{-2} s^{-1} which requires a dust mantle on the comets that would be at least 45 cm thick according to Fanale and Salvail[10], but perhaps 12 km thick according to Horányi *et al*[11]. The integral flux of our cometesimals is 7 orders of magnitude smaller than that of the Frank *et al.*[1] small comets.

A comparison of observations of Lyman-α made near 1 AU from OGO-5 and at ~1.35 AU from Mariner 9 shows that OGO-5 observed about 110 R more Lyman-α than Mariner 9 when the direction of observation from each was perpendicular to the Sun-spacecraft axis and downwind in the ISM[12]. From Fig. 1 the difference expected on the basis of the Voyager 2 observations and the $r^{-4.3}$ model is about 110 R. Although there are problems with comparing measurements made from different

spacecraft involving calibration and a possibility of contamination of the OGO-5 data from the geocorona, this comparison seems to support the results discussed in this paper.

We emphasize the many elements of uncertainty in this analysis. The data are sparse and scattered, and there is an unfortunate gap in the record between 1.033 AU to 1.3 AU. Thus, the radial dependence of Lyman-α is not well determined. (There will be an excellent opportunity to explore the entire region from 0.7 AU to 3 AU with the UVS on Galileo.) The treatment of hydrogen distribution in this paper neglects the smearing that is the consequence of cometary motion and the high velocity of the atoms produced by dissociation processes. Eventually, when and if a better data set becomes available, this effect should be taken into account. The r^{-2} dependence of $j(r)$ in equation (1) will always assure a rapid decrease in $4\pi I$ with r, however. The agreement with cratering data depends crucially on the density of the proposed cometesimals being very small. If their density should be as large as 0.25 g cm^{-3}, they would produce only 65 R of Lyman-α ($a > 1$ m). Whether the scaling law even applies to such low density impactors is not clear. It is possible that the sensitivity of the UVS decreased and then stabilized when the spacecraft was about 2×10^8 km from the Sun. This seems unlikely because there was no apparent change in sensitivity during the first 15 days of the mission when the first seven data points plotted in Fig. 1 were acquired. The model does require a surprisingly dramatic change in the Lyman-α productivity of these cometesimals very near 1 AU, but the ability of the model to explain the Lyman-α data and lunar crater density distribution is an appealing if not a compelling argument in its favour. Note that the cometesimals proposed here may have very clean icy surfaces and need not generate much dust. Hence, optical detection of even the largest may not be feasible. It would be worthwhile to try nevertheless.

We thank T. Ahrens and H. Masursky for useful information on cratering processes and lunar crater densities. This research was supported in part by the NSF and NASA.

Received 30 July; accepted 23 October 1987.

1. Frank, L. A., Sigwarth, J. B. & Craven, J. D. *Geophys. Res. Lett.* **13**, 307-310 (1986).
2. Donahue, T. M. *Geophys. Res. Lett.* **14**, 213-215 (1987).
3. Broadfoot, A. L. *et al. Space Sci. Rev.* **21**, 183-206 (1977).
4. Gombosi, T. I. & Houpis, H. L. F. *Nature* **324**, 43-44 (1986).
5. Hinteregger, H. E. *Adv. Space Res.* **1**, 39-52 (1981).
6. Thomas, G. *A. Rev. Earth planet. Sci.* **6**, 173-204 (1978).
7. Neukum, G. & Wise, D. V. *Science* **194**, 1381-1387 (1976).
8. Schmidt, R. M. & Housen, K. R. *Eos* **67**, 1078-1079 (1986).
9. Mendis, D. A. *Proc. 20th ESLAB Symp. Exploration Halley's Comet* (ESA SP-250, 1986).
10. Fanale, F. P. & Salvail, J. R. *Icarus* **60**, 476-511 (1984).
11. Horányi, M. *et al. Astrophys. J.* **278**, 449-455 (1984).
12. Bohlin, R. C. *Astr. Astrophys.* **28**, 323-326 (1973).

Vapour pressure of amorphous H_2O ice and its astrophysical implications

Akira Kouchi

Institute of Low Temperature Science, Hokkaido University, Sapporo 060, Japan

Because an understanding of the physical properties of vapour-deposited amorphous H_2O, I_{as}, is important for the discussion of the evolution of the Solar System[1-3], they have been extensively studied[4-9]. In particular, the importance of vapour pressure of I_{as} for the production rate of H_2O gas from a new comet has been realized[10,11]; but there has been no previous measurement of this. Here we present the results of experiments demonstrating that the vapour pressure of I_{as} is one or two orders of magnitude larger than that of crystalline H_2O and depends greatly on the condensation temperature, T_c, and the rate of condensation, R. We also discuss the evaporation of I_{as} in space.

A metal substrate in a vacuum chamber of 1×10^{-6} Pa (H_2O, 5×10^{-7} Pa; $N_2 + O_2$, 5×10^{-7} Pa) was cooled to T_c by continuous flow of liquid nitrogen. I_{as} was prepared by admitting H_2O vapour at room temperature into the vacuum system through a capillary tube of 1-mm diameter directed to a face of the substrate at a distance of 10 mm. The temperature of the substrate was controlled and measured with a Rh-Fe resistance thermometer mounted at the back of the substrate. Although the reading of the Rh-Fe sensor was calibrated in a separate experiment with Au-Fe7% Chromel thermocouples mounted at the surface of the substrate, we did not measure the temperature of the ice sample directly. The accuracy of the temperature measurement was ±0.5 K except for the temperature region near the phase transition of I_{as} to cubic ice, I_c, because the transition is exothermal. Under these conditions, the gas of H_2O monomer (revealed by the quadrupole mass spectrometer, QMS, Nichiden-Anelva AQS-360) immediately froze onto the substrate at a rate of 10^{2-3} nm h^{-1}. The deposition rates were measured by the interferometry of a He-Ne laser beam with the thin ice film. After deposition, the substrate was warmed up at a rate of 1 K min^{-1}. The sublimation rates of H_2O were measured with the QMS, which was calibrated by the standard H_2O leak. Vapour pressures were calculated by assuming that the vaporization coefficient, α_v, was close to unity[12-14]. The calculated vapour pressures were in good agreement with the reading of the calibrated ionization gauge (±5%) within ±10%. The precision of the absolute value of vapour pressure was not so good because of the assumption that $\alpha_v = 1$. But the sensitivity and stability of the QMS is very good, so any different results obtained for amorphous ice are significant.

Figure 1 shows the temperature dependence of vapour pressure of H_2O ice produced at various T_c and R. It is apparent that the vapour-pressure curve is divided into two parts. The low-temperature part is considered to correspond to I_{as}; the high-temperature part to I_c. The reasons are: first, previous studies show that I_{as} is formed by the precipitation of H_2O vapour onto the substrate at temperatures below 130-150 K[4]; second, because I_{as} is energetically unstable compared with I_c, the vapour pressure of I_{as} must be higher than that of I_c. Indeed, current experimental results agree with this prediction and with the thermodynamic estimation by Léger *et al.*[10]. This is the first clear report of the direct measurement of the vapour pressure of I_{as}.

The vapour pressure of I_{as} is found to be one or two orders of magnitude larger than that of I_c, and to vary systematically as functions of T_c and R. In general, when T_c is low and when R is small, the difference in vapour pressure between I_{as} and I_c is large. On the other hand, with increasing T_c and R the vapour pressure of I_{as} approaches that of I_c. The temperature differences between the curves of I_{as} and that of I_c under constant pressure, range from 10 to 20 K. This difference is larger than that estimated by Léger *et al.* (3-4 K)[10]. Figure 1 also shows the tendency for the slope of I_{as} to increase with decreasing T_c and R. Current experimental results suggest that the difference in vapour pressure between different samples of I_{as} is sensitive to structural differences. Thus we conclude that the structure of I_{as} cannot be determined uniquely by temperature but is highly dependent on condensation temperature and condensation rate.

In Fig. 1*a*, the data of Bryson *et al.*[14], whose T_c is rather high, 100 K, are also plotted. The two sets of data are fairly similar in the higher temperature part, but not in the low-temperature part. This comparison suggests (1) the accuracy of our measurement of vapour pressure is fairly good and (2) although they mentioned that the lower temperature part <150 K corresponds to I_{as}, we do not know whether it is amorphous or not.

Figure 2 shows the relationship between T_c and the crystallization temperature of I_{as}, T_x. The T_x, defined by the peak of I_{as},